Available online at www.sciencedirect.com
ScienceDirect
Journal of the European Ceramic Society 26 (2006) 3761–3768
www.elsevier.com/locate/jeurceramsoc

Effect of quartz particle size on the strength of triaxial porcelain

S.R. Bragança [a,*], C.P. Bergmann [a], H. Hübner [b]

[a] *Federal University of Rio Grande do Sul, LACER/UFRGS, Av. Osvaldo Aranha, 99/705, Porto Alegre 90135-190, Brazil*
[b] *Technical University of Hamburg-Harburg, 21071 Hamburg, Germany*

Received 12 August 2005; received in revised form 22 December 2005; accepted 6 January 2006
Available online 28 February 2006

Abstract

The effect of the quartz component on strength, σ_f, and fracture toughness, K_{Ic}, of a triaxial porcelain was studied by varying the size distribution of the quartz particles. Both σ_f and K_{Ic} were found to increase and then to pass over a maximum as the quartz distribution became finer. Improvements in σ_f and K_{Ic} of more than a factor of 2 were achieved. The flaw size that controlled failure was shown to equal the maximum quartz particle size in the material containing the coarsest quartz component and to be a constant independent of the quartz size in the other materials. The toughness increase was attributed to microcrack toughening of the glass matrix, the microcracks being formed by thermal mismatch stresses between the quartz particles and the glass matrix on cooling from the sintering temperature.
© 2006 Elsevier Ltd. All rights reserved.

Keywords: Porcelain; Strength; Toughness; Microstructure; Quartz

1. Introduction

The mechanical properties of ceramics are strongly controlled by their microstructure. In the case of triaxial porcelains, the strength of the final product is the result of a complex interaction of a series of processing parameters such as the characteristics and composition of the starting materials, the conditions of mixing and forming, and the details of sintering, e.g. the furnace atmosphere and the ramp, soak temperature and duration of the heating cycle. The reason is that these factors largely determine the evolution of the microstructure and the formation and development of phases during sintering. The variables involved can barely be controlled in an adequate manner, which makes it difficult to predict the final properties of a porcelain with a reasonable degree of reliability.

The principal factor to influence the strength of triaxial porcelains is considered to be the size of the quartz particles as has been shown repeatedly by several researchers.[1–6] The present study was undertaken with the aim to further elucidate the effect of the quartz phase on the mechanical properties of triaxial porcelains. For that, various batches of a hard porcelain were fabricated that differed in the quartz particle size, with all other processing parameters being kept constant. Strength and fracture toughness were determined experimentally and the resulting flaw size was compared with the size of the largest quartz particles. It could be shown that the flaw size of the materials studied did not correlate with the maximum particle size, but was controlled instead by thermally induced microcracks between crystalline particles and the glass matrix.

1.1. The strength of ceramics

The fundamental concept of the fracture strength of ceramics has been developed mainly by Davidge and Evans.[7,8] It combines the basic idea of stress concentrations around flaws which has been presented by Griffith in 1920 with the principles of Linear Elastic Fracture Mechanics developed in the 1940s. As summarized in Ref.[8], the basic equation of the fracture strength of ceramics is given by

$$\sigma_f = \frac{1}{Y}\left[\frac{2\gamma_i E}{c}\right]^{1/2} \quad (1)$$

where σ_f is the fracture strength, γ_i effective surface energy or fracture energy for crack initiation, E Young's modulus, c the flaw size, and Y the Fracture Mechanics calibration factor. Eq. (1) is the Griffith equation. According to Fracture Mechanics,

* Corresponding author. Tel.: +55 51 33163405; fax: +55 51 33163405.
E-mail address: saulorb@ufrgs.br (S.R. Bragança).

0955-2219/$ – see front matter © 2006 Elsevier Ltd. All rights reserved.
doi:10.1016/j.jeurceramsoc.2006.01.012

the critical stress intensity factor of a material, K_{Ic}, is given by

$$K_{Ic} = Y\sigma_f c^{1/2} \quad (2)$$

The calibration factor Y takes into account the limited dimensions of a test piece and depends on the loading geometry. For the case of four-point bending as used in the present work, the calibration function was given for the first time by Gross and Srawley[9] in 1965:

$$Y = 1.99 - 2.47\left(\frac{c}{w}\right) + 12.97\left(\frac{c}{w}\right)^2 - 23.17\left(\frac{c}{w}\right)^3 + 24.8\left(\frac{c}{w}\right)^4 \quad (3)$$

where w is the width of the bending bar. From Eqs. (1) and (2) it can easily be seen that the fracture energy for crack initiation, γ_i, and the critical stress intensity factor, K_{Ic}, are connected by the relationship

$$K_{Ic} = (2\gamma_i E)^{1/2} \quad (4)$$

Following Evans and Davidge,[7,8] it becomes clear from the foregoing set of equations that the strength of a ceramic body is controlled by two fundamental parameters, i.e. the flaw size c and the critical stress intensity factor K_{Ic}. The latter may be substituted by the fracture energy γ_i. These two parameters were used in the present work in order to characterise the mechanical behaviour of the triaxial porcelains studied.

The critical stress intensity factor (or fracture toughness) may be considered to represent the intrinsic capability of a brittle material to withstand crack initiation and crack propagation when subjected to mechanical loading. Additional contributions to the stress intensity factor may be caused by internal features such as the mode of fracture, i.e. inter- or transcrystalline crack propagation, the action of internal stresses, the presence of reinforcing elements and the strength of bonding between phases in multiphase or glass-containing microstructures. The flaw size, on the other hand, is given by the largest inhomogeneity of the microstructure that causes a stress concentration under loading. Fracture-initiating defects may be any kinds of inherent irregularities on a microstructural level as for example residual pores, exaggerated grains, microscopic surface scratches, broken grain boundaries and small impurity particles. If all these defects are avoided the proper grain size, i.e. the largest grains may be the strength-limiting defects.[8] The aim in developing a ceramic of a high strength in the brittle temperature regime therefore is to provide a fracture toughness as high as possible and to avoid any microstructural inhomogeneities as far as possible. The results of the present study will be discusses in terms of this concept.

2. Experimental procedure

Eight different types of a triaxial porcelain were fabricated which exhibited identical fractions of clay, flux and filler in a traditional ratio, i.e. 50% of kaolin, 25% of feldspar and 25% of quartz, but different size distribution of the quartz component. The quartz powder was a commercial silica (SIBELCO Co., Jaguaruna, Brazil) with an average particle size of 100 μm.

Table 1
Chemical composition of the starting materials

	Kaolin (%)	Feldspar (%)	Quartz (%)
SiO_2	46.96	67.02	99.81
Al_2O_3	38.05	19.22	0.12
Fe_2O_3	0.46	0.19	0.08
MnO	0.008	0.007	0.002
MgO	0	0	0.01
CaO	0.02	0.06	0.01
Na_2O	0.03	3.75	0.03
K_2O	1.14	9.42	0.06
TiO_2	0.03	0	0.073
P_2O_5	0.108	0.035	0.02
LOI	13.2	0.3	0.1
Total	99.9	100	99.9

Both kaolin and feldspar were raw materials used in the porcelain industry for tile production (Cerâmica Eliane, Cocal do Sul, Brazil). The chemical composition of these materials was analyzed by X-ray fluorescence. The results are summarized in Table 1. It can be seen that the materials had low levels of impurities such as Fe_2O_3, which makes them very suitable for the fabrication of white porcelains. Crystalline phase analysis by X-ray diffraction of the kaolin showed the presence of kaolinite ($Al_2Si_2O_5(OH)_4$ as the main phase and muscovite ($KAl_2(AlSi_3O_{10})(OH)_2$) and illite ($KAl_3Si_3O_{10}(OH)_2$) as secondary phases, whereas the feldspar was found to be mainly composed by microcline ($KAlSi_3O_8$) and albite ($NaAlSi_3O_8$).

Quartz powders of reduced particle size were obtained by wet ball milling the starting powder grade A during different milling times up to 50 min using agate balls. Grade D was sieved prior to milling to pass mesh 150 and grade F, G and H to pass 325 mesh. Exceptionally, Grade E was dry milled to 60 min. Thus, additionally to the original quartz powder (grade A), seven further powders of finer particle size were obtained (grades B to H). Subsequently, the size distribution was determined in a laser particle size analyzer (CILAS model 1180, Company Industrielle des Lasers, Orléans, France). Table 2 summarizes characteristic size data of these eight powders.

Figs. 1 and 2 show histograms and the sum frequency of the particles of grades A and H, i.e. the coarsest and the finest quartz powder of the series. According to Table 2, a significant variation of the particle distribution was achieved. The attention should be drawn at the large particle diameters since they are likely to control the strength of the sintered bodies. On comparing the coarse-grained grade A and the fine-grained grade H, both the diameters of the largest 10% fraction and the maximum diameters, d_{max}, differ by a factor of more than 30. Furthermore, a considerable amount of small particles was found to be present in each of the eight quartz grades. It can be expected, therefore, that the small particles will be dissolved in the glass phase during sintering and that liquid-phase attack of the large particle will be small, specifically at short sintering times.

Employing the quartz filler grades A to H of Table 2, eight different batches A to H of porcelain were prepared by mixing and uniaxial semi-dry pressing of the starting powders into test bars. A small amount of 2.5% of an organic binder (polyvinyl

Table 2
Size distribution of quartz particles

Material	Milling time (min)	Particle diameter, d (μm), at a sum frequency of			Mean diameter, $\bar{d}$ (μm)	Maximum diameter d_{max} (μm)
		10%	50%	90%		
Grade A	–	37.1	97	168	101	≈400
Grade B	7.5[a]	2.8	34	104	45	≈270
Grade C	10	4.5	47	70	43	≈140
Grade D	25	3.6	32	48	30	≈75
Grade E	60[b]	0.9	4.1	18.7	7.2	≈50
Grade F	40[a]	1.0	5.1	17.2	7.4	≈32
Grade G	40	1.2	6.8	19	8.7	≈31
Grade H	50	0.9	2.3	5.5	2.8	≈11

[a] 2° Batch.
[b] Dry milled.

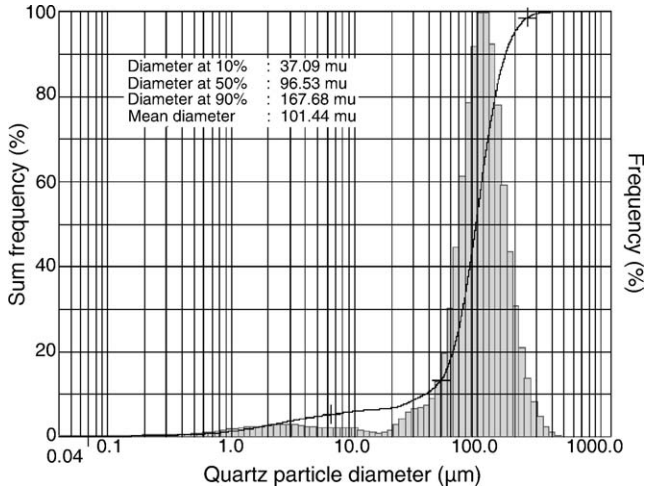

Fig. 1. Histogram and sum frequency of the size distribution of quartz particles of grade A (as-received).

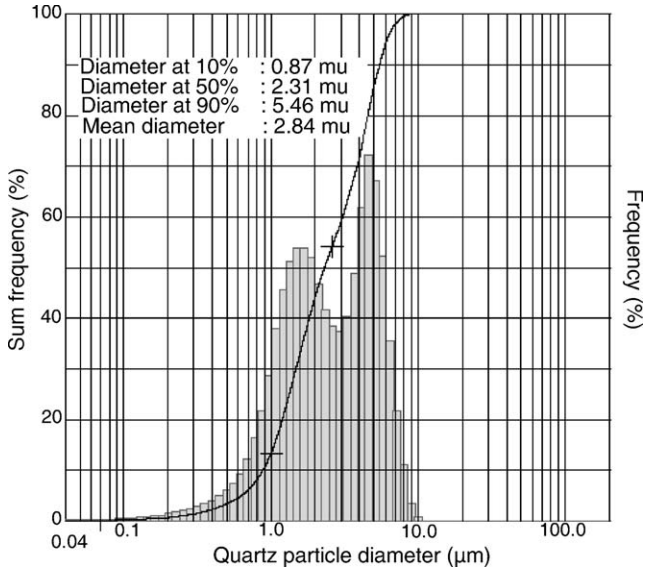

Fig. 2. Histogram and sum frequency of the size distribution of quartz particles of grade H (after 50 min of ball milling).

alcohol) was added to prevent fracture of the pressed pieces. The green bodies were dried in air and sintered in an electric laboratory furnace. The furnace was heated with a temperature ramp of 150 °C/h until the sintering temperature of 1340 °C was reached. The time at temperature was 30 min, and cooling occurred along the natural cooling rate of the furnace. Test bars of the dimensions 7 mm × 7 mm × 60 mm were produced for strength and fracture-toughness testing. The test bars for K_{Ic} testing were notched to a depth between 1 and 2 mm with a diamond saw blade of 0.3 mm width. This method is generally assumed to generate sharp microcracks at the root of the notch. Fig. 3 shows the side face of a notched specimen.

Both strength and fracture toughness were measured in four-point bending. The determination of the bend strength was carried out according to the measuring standard ASTM C-133/97, but employing a somewhat smaller cross-head speed of the testing machine of 0.5 mm/min only. The strength σ_f was calculated from the expression

$$\sigma_f = \frac{3}{2}\frac{P_{max}(L-\ell)}{bw} \quad (5)$$

where P_{max} is the load at fracture, L and ℓ are the lower and upper span length, and b the height of the specimen. The frac-

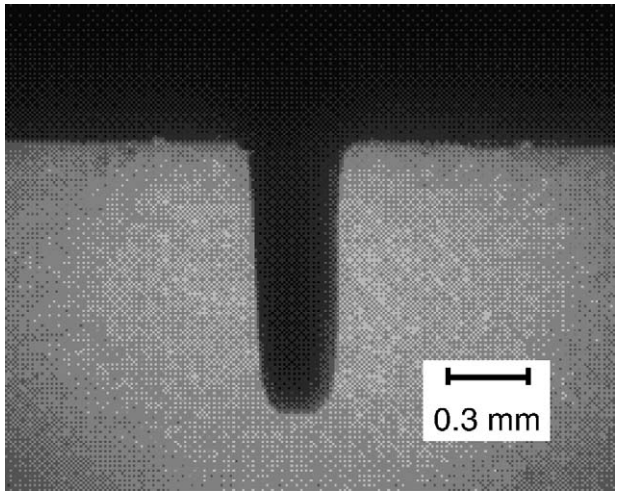

Fig. 3. Notched specimen.

Table 3
Fracture toughness and strength data

	Number of specimens	Fracture toughness K_{Ic} (MPa m$^{1/2}$)	Fracture energy γ_i (J/m^2)	Number of specimens	Fracture strength σ (MPa)	Flaw size range, c (μm)
Grade A	6	0.67 ± 0.05	2.9 ± 0.4	6	19.8 ± 1.6	270–430
Grade B	8	0.76 ± 0.11	4.1 ± 1.2	8	30.2 ± 1.9	180–240
Grade C	9	0.77 ± 0.05	3.8 ± 0.5	7	28.9 ± 1.7	170–230
Grade D	6	0.95 ± 0.06	5.9 ± 0.8	6	36.2 ± 2.5	150–220
Grade E	10	1.38 ± 0.14	13.3 ± 2.7	10	52.6 ± 5.6	150–250
Grade F	12	1.54 ± 0.08	16.5 ± 1.6	11	58.6 ± 4.3	155–245
Grade G	8	1.44 ± 0.14	13.5 ± 2.9	8	62.0 ± 7.8	100–250
Grade H	8	1.32 ± 0.10	12.1 ± 1.7	7	54.5 ± 3.8	130–200

ture toughness K_{Ic} was calculated from Eqs. (2) and (3). The fracture energy γ_i was obtained from K_{Ic} by means of Eq. (4) using $E = 78$ GPa for Young's modulus as suggested by Mattyasovszky-Zsolnay.[10]

3. Results

Strength and fracture toughness data of the eight materials batches are summarized in Table 3. It shows the number of specimens tested and the mean value of K_{Ic} and σ_f obtained, together with the standard deviation. Data of the fracture energy, γ_i, and the flaw size, c, as calculated by means of Eqs. (4) and (1), respectively, are also listed.

Fig. 4 is a plot of K_{Ic} and σ_f versus composition. It shows that both fracture toughness and strength are substantially affected by the type of the quartz component. As the size of the quartz particle distribution becomes finer, both parameters are increased markedly, pass through a maximum, and finally diminish a bit. This finding demonstrates that there is an optimum composition with respect to maximum strength, i.e. at grades F and G. Furthermore, K_{Ic} and σ_f seem to be influenced by the quartz addition in much the same way since in batches B to H, both quantities exhibit a nearly parallel variation with composition. Only in grade A, there seems to be a major deviation in the development of strength and K_{Ic}. This observation may be evidence that the flaw size in grades C to H is not much affected by the quartz particle size distribution, as will be discussed later.

From Table 3 and Fig. 4 it can be seen that only grades E to H achieved K_{Ic} values above 1 MPa m$^{1/2}$. The particle distributions with diameter 90% smaller than ~19 μm (see Table 2) achieved the higher K_{Ic}. These numbers are very close to those reported by other authors. K_{Ic} data in the range of 1–2 MPa m$^{1/2}$ were suggested by Freiman.[11] The data reported by Batista et al.[12] are 1.4 ± 0.04 MPa m$^{1/2}$ for a hard porcelain containing alumina as a filler and 2.3 ± 0.2 MPa m$^{1/2}$ for bone china. The K_{Ic} value found in a previous study by two of the present authors[6] was 1.6 MPa m$^{1/2}$. Thus, the results of grades E and H seem to be common for porcelains containing quartz additives.

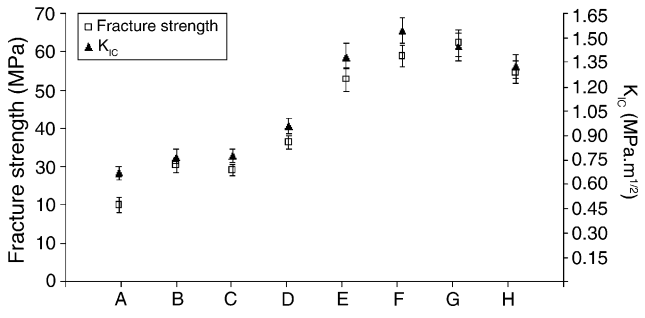

Fig. 4. Fracture toughness and fracture strength of the 8 batches tested.

The K_{Ic} data of grades A to D, however, are less satisfactory. It has been pointed out by several authors[2,5] that a mean filler particle size of 30 μm should be the best choice to achieve optimum strength. Looking at the quartz particle distributions of Table 2 it can be seen that even batch D, despite of a mean particle size of only 30 μm, still contains a 10% fraction larger than 48 μm, which is thought to be responsible for the low fracture toughness.

Strength data similar to those listed in Table 3 were found also in other studies. Warshaw and Seider[2] reported strength values of 65 MPa for a porcelain containing quartz and 120 MPa for a porcelain containing alumina as a filler material, respectively. According to Kingery et al.,[13] the strength of mullite porcelain is 69 MPa. In two further studies of the effect of filler size on the strength of porcelain, a maximum value of 52 MPa was reported by Carty and Pinto,[14] whereas a range from 60 to 110 MPa was found by Andreeva and Ordan'yan.[15] Thus, the strength data measured in this work compare well with those reported in similar studies.

4. Discussion

An attempt will be made in the following to interpret the findings described in the foregoing paragraphs, specifically (1) the strong effect of the filler size distribution on both strength and fracture toughness, and (2) the observation that both of the mechanical properties were influenced in a very similar way.

As shown in Figs. 1 and 2 and in Table 2, the diameters of the eight quartz-starting powders were distributed over a wide size range, beginning with particles in the range of some tenth of a micron up to the maximum diameter d_{max} between around 10 to several 100 μm. It has been pointed out that the quartz component of porcelain glasses is dissolved into the glass phase during sintering until a saturation limit is reached in the glass so that the dissolution comes to an end.[14,16] It must be noted, however, that the dissolution rate of the quartz is size-dependent. It varies with $1/d$ with d the particle diameter, as predicted by the Kelvin

equation. It is expected, therefore, that the smaller particles will be dissolved at a faster rate and, under the sintering conditions of this study, disappear before the larger particles will undergo a major size reduction, as has also been found experimentally.[14] On the other hand, it is exactly the particle population at the upper end of the size distribution that is expected to affect the mechanical behaviour.

4.1. Strength

As discussed previously, the strength of ceramics is controlled by two basic parameters, which are the fracture toughness and the fracture-initiating flaw. In a first approach to elucidate the strength-controlling mechanism in the porcelains of this study, the flaw size was calculated by means of Eq. (1) for each broken specimen. For that, the K_{Ic} value measured for each batch was used for the expression $(2\gamma_i E)^{1/2}$ in the numerator of Eq. (1). Thus, the calculated flaw size becomes independent of the value of Young's modulus, which was not determined in this study. A value of $Y=2$ was used for the Fracture Mechanics calibration factor. The flaw size range found for the range of strength values of each batch is plotted in Fig. 5. The figure also contains the range of the quartz particle size distribution as obtained from the particle size analyzer measurements such as those shown in Figs. 1 and 2. At the upper end of the quartz particle size distribution of Fig. 5 the maximum particle diameter d_{max} is reached. The figure demonstrates that in the grades A and B porcelains which contains the largest filler particles the flaw size equals the maximum particle size:

$$c \approx d_{max}, \quad \text{in grades A and B} \tag{6}$$

It is concluded, therefore, that in these materials the largest quartz particles act as the strength-controlling defects. They are thought to form pre-existing flaws of the length of the maximum particle size that lead to failure. The maximum residual stress in quartz grains was found for quartz particle size of ~90 μm according to Carty and Pinto,[14] and correlates well with the results of Table 3.

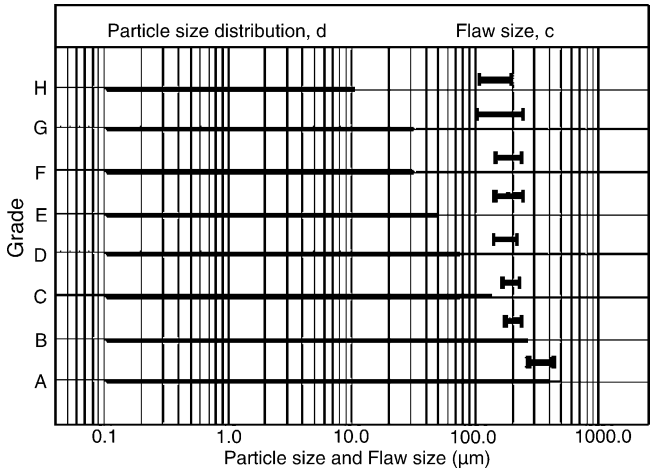

Fig. 5. Comparison between quartz particle size, d, and flaw size, c.

In grades C to H, however, the flaw size comes out to be distinctly larger than the size of the largest filler particles and is found to be essentially a constant independent of the upper bound of the quartz particle size distribution, i.e.

$$c \approx const. > d_{max}, \text{ in grades C to H} \tag{7}$$

Here the flaw size is around 100–250 μm. This figure should be compared with d_{max} which lies between 11 μm (grade H) and 140 μm (grade C). The largest deviation between the failure-initiating defect and the largest microstructural inhomogeneity is observed in grade H material where the ratio of the flaw size to the maximum quartz particle size is $c/d_{max} \approx 200\,\mu m/11\,\mu m \approx 18$. Thus, it is concluded that substantial crack growth and/or crack linking must have occurred prior to failure.

The origin of the large strength-controlling defects plotted in Fig. 5 must be seen in the presence of microcracks that are frequently observed in porcelains containing quartz as a filler material. Microcracks around quartz particles were reported by Mattyasovszky-Zsolnay,[10] Warshaw and Seider,[2] Schüller,[17] Kobayashi et al.,[3] Carty and Senapati,[18] Ohya and Takahashi,[4] and Ece and Nakagawa.[5] Agreement exists about the cause of microcrack generation in porcelain. Due to the high thermal expansion coefficient of quartz and the low coefficient of the glass matrix, stresses are set up within and around the quartz particles upon cooling from the sintering temperature. The phase transformation of the quartz may also be an important reason for the formations of microcracks.

According to Davidge,[8] a radial tensile stress is built up in the particle and in the surrounding matrix, as well as a tangential tensile stress in the particle and a tangential compressive stress in the matrix at the interface. At a stress level sufficiently high, this stress field should create transversal cracks within the particles and circumferential cracks around them. An assessment of the stress within a quartz particle was made to show if microcracking is likely to occur in the materials of this study. The magnitude of the tensile stress due to thermal mismatch in a quartz particle, σ_{qu}, is given in Eq. (8) by the relationship,[8]

$$\sigma_{qu} = \frac{\Delta\alpha\Delta T}{(1+\nu_{gl}/2E_{gl}) + (1-2\nu_{qu}/E_{qu})} \tag{8}$$

where $\Delta\alpha = \alpha_{qu} - \alpha_{gl}$ is the difference of the thermal expansion coefficients of quartz and glass, ΔT the temperature range of cooling, ν_{gl} and ν_{qu} are Poisson's ratios of glass and quartz, respectively, and E_{gl} and E_{qu} the elastic moduli of the two components. Eq. (8) was used to assess the stress level induced in our materials. For that, the following numbers were used, as suggested in Ref.[10]: $\alpha_{qu} = 23 \times 10^{-6}$ 1/K and $\alpha_{gl} = 3 \times 10^{-6}$ 1/K for the temperature range from 750 °C to 20 °C, $\Delta T = 730$ °C, $\nu_{gl} = \nu_{qu} = 0.2$, and $E_{gl} = E_{qu} = 78.4$ GPa. This yields $\sigma_{qu} \approx 950$ MPa for the tensile stress in a quartz particle.

A tensile stress of this magnitude should be able to create transversal cracks both within the quartz particles and in the glass matrix. In fact, such microcracks were detected in this study, too. The following four figures are scanning electron micrographs of

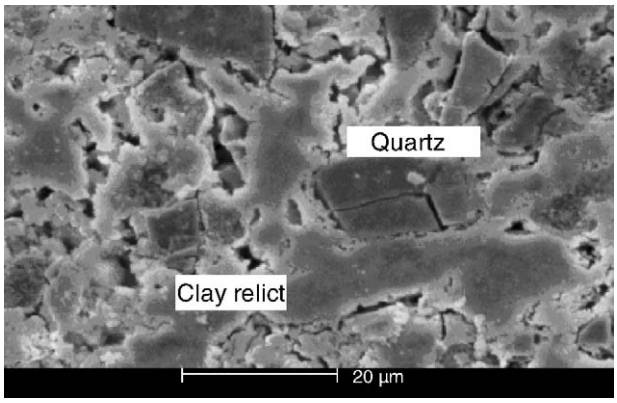

Fig. 6. SEM micrograph of grade D material showing intragranular cracks within a quartz particle.

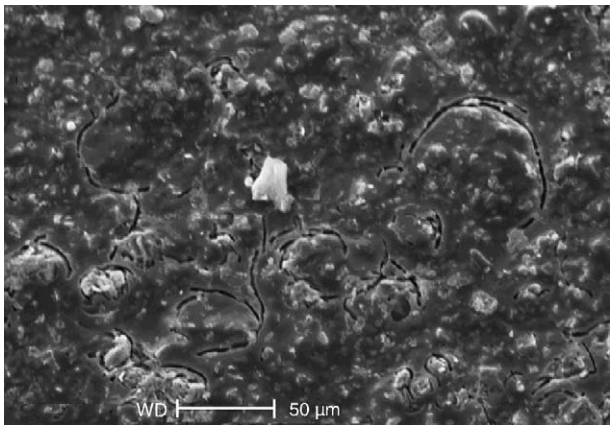

Fig. 8. SEM micrograph showing matrix cracks in grade G porcelain.

porcelain surfaces. In Figs. 6 and 7, quartz particles embedded in grade C porcelain are shown that exhibit a transversal crack and a circumferential crack, respectively. The particle size is about 20 μm in Fig. 6 and 35 μm in Fig. 7. In both of the cases, the specimen surface was polished and subsequently etched with 20% hydrofluoric acid. The particle of Fig. 6 is completely fractured into at least two or perhaps even three parts, whereas the particle of Fig. 7 is completely surrounded by a number of interconnected small cracks.

The micrographs of Figs. 8 and 9 were taken from an as-received specimen surface of grade G material and show a series of curved microcracks within the glass matrix. The microcracks of Fig. 8 have typical extensions between 25 and 80 μm, those of Fig. 9 lie in the range between about 15 and 40 μm. These observations demonstrate that matrix cracks could be found the size of which considerably exceeded the maximum quartz particle size ($d_{max} \approx 31$ μm). Microcracks were also found in the other porcelains grades, even in the material H, but at a lower extent. It is noted, however, that the probability to find microcracks of a larger extension was higher in materials of a larger quartz particle size, in agreement with observation reported elsewhere.[2]

The SEM study revealed that numerous microcracks could be detected in the porcelains investigated. They are considered to be the pre-existing defects of these materials. They are thought to grow from the subcritical size up to a failure-initiating extension upon loading. On growing, they may join with other microcracks and link together until they extend to a flaw that is critical in terms of the Griffith equation, Eq. (1). Such linking mechanisms in ceramics were suggested by several authors, e.g. by Davidge and Evans[7] and by Meredith and Pratt.[19]

Summing up it is noted that the effect of the quartz particle size on the strength of our porcelains can be understood when the development of the fracture-initiating flaw is considered. In materials of grade C to H, flaws of a constant size form during loading (Fig. 5). They start from pre-existing microcracks and extend by subcritical crack growth and/or crack linking. The variation of the strength with the type of the quartz powder (Fig. 4) is due to the variation of K_{Ic}. In the grades A and B materials containing the coarsest quartz powder, on the other hand, the largest quartz particles present in the microstructure serve as the fracture-initiating flaws.

4.2. Toughness

On discussing the effect of the quartz particle population on K_{Ic}, two findings must be considered: (1) the strong effect of the quartz size on K_{Ic} that was found to increase by a factor of more

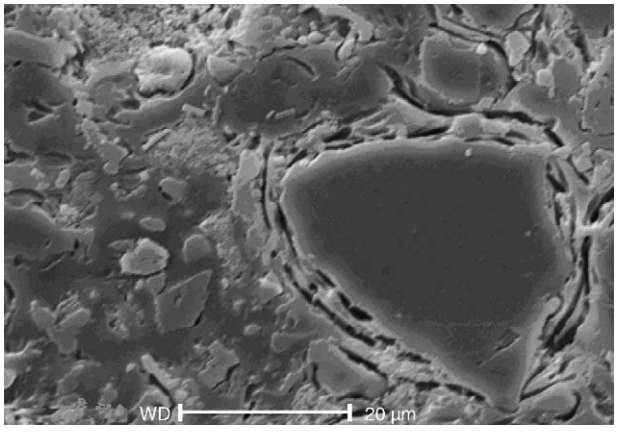

Fig. 7. SEM micrograph of grade D material showing circumferential cracks around a quartz particle.

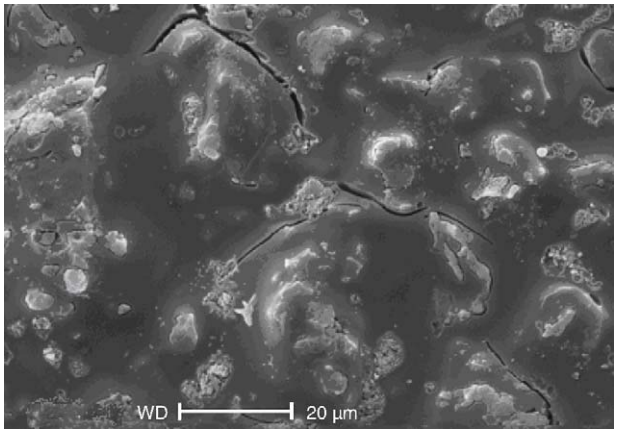

Fig. 9. SEM micrograph showing matrix cracks in grade G porcelain at a higher magnification.

than 2 (Table 3 and Fig. 4) and (2) the formation of microcracks in the glass matrix of all grades studied (Figs. 8 and 9). It is believed that the two effects are not independent of each other. Rather, the toughness increase is attributed to an increase in the number of microcracks.

Microcrack toughening has been proposed repeatedly as a strengthening mechanism in ceramics, e.g. by Evans and Fu.[20] Microcracks are believed to add to the fracture toughness due to different effects. One explanation is that microcracks modify the stress-strain characteristics of the region ahead the crack tip since they reduce the elastic modulus within this zone. This results in distributing the external stress over a larger volume, thereby shielding the tip from the applied stress. Thus, in order to initiate fracture, a higher stress must be applied which results in an enhancement of the resistance against fracture, i.e. the fracture toughness. Another kind of view is that microcracks in the highly stressed region ahead the main crack may grow by subcritical crack growth. This process contributes to absorb stored elastic energy necessary to propagate the main crack, thereby increasing the fracture toughness.

The local stresses to create microcracks can be set up by the mismatch of two phases, e.g. second-phase particles embedded in a matrix. The mismatch may be either due to a different thermal expansion (stress-induced microcracking) or to a phase transformation with a volume change (transformation-induced microcracking), such as transformation toughening of ceramic matrices by zirconia particles.

Stress-induced microcracking was reported not only for polycrystalline ceramics, but also for glass matrix systems. For a borosilicate glass containing dispersed alumina particles a toughness increase by a factor of 2 was found by Faber et al.[21] and attributed to stress-induced microcracking. The formation of microcracks in the porcelains of this study is thought to be stress-induced, too. It was shown in the foregoing discussion that the thermal mismatch between a quartz particle and the surrounding glass matrix is sufficiently high to create a local stress of nearly 1000 MPa.

Assuming the toughness increase of Fig. 4 to be caused by microcracks, the variation of K_{Ic} with the refinement of the quartz distribution can be explained at least quantitatively. The essential feature in the mechanism of microcrack toughening is the microcrack density that means the number of microcracks per unit volume. To generate a microcrack, the quartz particle must have a minimum size. Particles of a diameter d larger than a critical value d_{crit} will be able to generate a crack, whereas smaller particles will not. Hence, only a fraction of the total number is expected to generate microcracks. It can be assumed, therefore, that the microcrack density will increase as the number of particles per unit volume having a size $d > d_{crit}$ increases. Proceeding from porcelain grade A to grade E the quartz distribution is shifted more and more to smaller sizes. Since the volume fraction of the quartz phase was kept constant the total number of particles per unit volume, i.e. the particle density, increases from grade A to grade E. This increase can be considerable because much more particles are necessary to build up the given volume fraction when their size is reduced. As a consequence, the particle fraction having a size $d > d_{crit}$ is expected to increase, and so will the microcrack density and, hence, the fracture toughness K_{Ic} as in fact was found. Proceeding from grade G to grade H, the increase in particle density may be compensated by the decrease of the particle size, leading to the slight fall of K_{Ic}.

5. Conclusions

It was demonstrated that the strength and the fracture toughness of a triaxial porcelain can be increased markedly by the addition of a 25 wt% quartz component as a filler material. By a suitable choice of the size distribution of the quartz particles, both σ_f and K_{Ic} could be improved by a factor of 2–3. The improvement can be explained by the mechanism of microcrack toughening, the microcracks being generated by the thermal mismatch between the crystalline quartz particles and the glass matrix. Failure was shown to originate at the largest particles of the distribution. Thus, cutting the upper end of the size distribution resulted in a reduction of the failure-initiating flaw size.

Acknowledgement

Financial support from CNPq is gratefully acknowledged.

References

1. Kane, S. C. and Cook, R. L., Effect of grinding and firing treatment on the crystalline and glass content and physical properties of whitewares bodies. *J. Am. Ceram. Soc.*, 1951, **34**, 145–151.
2. Warshaw, S. I. and Seider, R. J., Comparison of strength of triaxial porcelains containing alumina and silica. *J. Am. Ceram. Soc.*, 1967, **50**, 337–342.
3. Kobayashi, Y., Ohira, O. and Kato, E., Effect of firing temperature on bending strength of porcelains for tableware. *J. Am. Ceram. Soc.*, 1992, **75**, 1801–1806.
4. Ohya, Y. and Takahashi, Y., Acoustic emission from a porcelain body during cooling. *J. Am. Ceram. Soc.*, 1999, **82**, 445–448.
5. Ece, O. I. and Nakagawa, Z., Bending strength of porcelains. *Ceram. Int.*, 2002, **28**, 131–140.
6. Bragança, S. R. and Bergmann, C. P., A view of whitewares mechanical strength and microstructure. *Ceram. Int.*, 2003, **29**, 801–806.
7. Davidge, R. W. and Evans, A. G., The strength of ceramics. *Mater. Sci. Eng.*, 1970, **6**, 281–298.
8. Davidge, R. W., *Mechanical Behaviour of Ceramics*. Cambridge University Press, Cambridge, 1979.
9. Gross, B. and Srawley, J.E., Stress-intensity factors for single-edge-notch specimens in bending or combined bending and tension by boundary collocation of a stress function. NASA TN D-2603, 1965.
10. Mattyasovszky-Zsolnay, L., Mechanical strength of porcelain. *J. Mater. Sci.*, 1957, **40**, 299–306.
11. Freiman, S. W., Fracture mechanics: applications for whitewares. In *Science of Whitewares*, ed. V. E. Henkes, G. Y. Onada and W. M. Carty. The American Ceramic Society, Westerville, USA, 1996, pp. 293–304.
12. Batista, S. A., Messer, P. F. and Hand, R. J., Fracture toughness of bone china and hard porcelain. *Br. Ceram. Trans.*, 2001, **100**, 256–259.
13. Kingery, W. D., Bowen, H. K. and Uhlmann, D. R., *Introduction to Ceramics (2nd ed.)*. John Wiley & Sons, New York, 1976, p. 791.
14. Carty, W. M. and Pinto, B. M., Effect of filler size on the strength of porcelain bodies. *Ceram. Eng. Sci. Proc.*, 2002, **23**(2), 95–104.
15. Andreeva, N. A. and Ordan'yan, S. S., Technological implications in increasing the strength of porcelain. *Refractories Ind. Ceram.*, 2002, **43**, 325–328.
16. McConville, C. J., Shah, A. and Carty, W. M., Quartz dissolution into porcelain glasses. In *Whitewares and Materials, Ceramic Engineering and Science Proceedings*, *Vol. 25, Issue 2*, ed. W. M. Carty. The American Ceramic Society, Westerville, USA, 2004, pp. xy–yz.

17. Schüller, K. H., *Porcelain. Ceramics Monographs—Handbook of Ceramics*. Verlag Schmidt GmbH, Freiburg, 1979.
18. Carty, M. W. and Senapati, U., Porcelain—raw materials, processing, phase evolution, and mechanical behavior. *J. Am. Ceram. Soc.*, 1998, **81**, 3–20.
19. Meredith, H. and Pratt, P. L., The observed fracture stress and measured values of K_{Ic} in commercial polycrystalline alumina. *Special Ceramics* 6. *Br. Ceram. Res. Assoc.*, 1975, 107–122.
20. Evans, A. G. and Fu, Y., Some effects of microcracks on the mechanical properties of brittle solids. 2. Microcrack toughening. *Acta Met.*, 1985, **33**, 1525–1531.
21. Faber, K. T., Iwagoshi, T. and Ghosh, A., Toughening by stress-induced microcracking in two-phase ceramics. *J. Am. Ceram. Soc.*, 1988, **71**, C399–C401.